Bone xxx (2011) xxx–xxx

Contents lists available at ScienceDirect

Bone

journal homepage: www.elsevier.com/locate/bone

Development of micro-CT protocols for *in vivo* follow-up of mouse bone architecture without major radiation side effects

K. Laperre [a,1], M. Depypere [b,1], N. van Gastel [a], S. Torrekens [a], K. Moermans [a], R. Bogaerts [c], F. Maes [b], G. Carmeliet [a,*]

[a] *Laboratory of Experimental Medicine and Endocrinology, K.U.Leuven, Leuven, Belgium*
[b] *ESAT/PSI, Medical Image Computing, K.U.Leuven, Leuven, Belgium*
[c] *Experimental Radiotherapy Section, K.U.Leuven, Leuven, Belgium*

ARTICLE INFO

Article history:
Received 29 December 2010
Revised 26 May 2011
Accepted 24 June 2011
Available online xxxx

Edited by: Harry Genant

Keywords:
In vivo micro-CT
Skeletal system
Bone architecture
Radiation toxicity
Image quality

ABSTRACT

In vivo micro-computed tomography (micro-CT) will offer unique information on the time-related changes in bone mass and structure of living mice, provided that radiation-induced side effects are prevented. Lowering the radiation dose, however, inevitably decreases the image quality. In this study we developed and validated a protocol for *in vivo* micro-CT imaging of mouse bone architecture that retains high quality images but avoids radiation-induced side effects on bone structure and hematological parameters.

The left hindlimb of male C57Bl/6 mice was scanned *in vivo* at 3 consecutive time points, separated each time by a 2-week interval. Two protocols for *in vivo* micro-CT imaging were evaluated, with pixel sizes of 9 and 18 μm and administered radiation doses of 434 mGy and 166 mGy per scan, respectively. These radiation doses were found not to influence trabecular or cortical bone architecture in pre-pubertal or adult mice. In addition, there was no evidence for hematological side effects as peripheral blood cell counts and the colony-forming capacity of hematopoietic progenitor cells from bone marrow and spleen were not altered. Although the images obtained with these *in vivo* micro-CT protocols were more blurred than those obtained with high resolution (5 μm) *ex vivo* CT imaging, longitudinal follow-up of trabecular bone architecture in an orchidectomy model proved to be feasible using the 9 μm pixel size protocol in combination with a suitable bone segmentation technique (*i.e.* local thresholding). The image quality of the 18 μm pixel size protocol was too degraded for accurate bone segmentation and the use of this protocol is therefore restricted to monitor marked changes in bone structure such as bone metastatic lesions or fracture healing.

In conclusion, we developed two micro-CT protocols which are appropriate for detailed as well as global longitudinal studies of mouse bone architecture and lack noticeable radiation-induced side effects.

Introduction

In vivo micro-computed tomography (micro-CT) has been suggested as a valuable tool to monitor local changes in bone structure in living mice [1]. This technology can offer unique high resolution information on the temporal responses of specific bone regions to pathological or therapeutic stimuli, stipulated that the micro-CT imaging process itself has no influence on the skeletal system. Indeed, frequent or excessive exposure of the skeletal system to X-rays leads to side effects which are closely related to the radiation dose and include growth retardation, skeletal deformities, bone loss and hematological abnormalities [2,3].

Radiation can cause cell death, most likely as a consequence of irreparable DNA damage [4,5]. But also low radiation doses can result in non-lethal DNA damage, which will initiate DNA repair processes and ultimately lead to a decrease in cell proliferation [6]. It is therefore generally accepted that proliferating cells are more radiosensitive than non-proliferating cells and that less differentiated cells are more prone to radiation damage than highly differentiated cells [7]. This radiation-induced cytotoxicity has resulted in the use of radiation as a local therapy for numerous malignancies in humans.

Radiation will also harm non-malignant cells and several studies have investigated the effects of high-dose radiation on bone cells *in vitro* and *in vivo*. X-ray radiation in the range of 2.5 to 8 Gy inhibits the proliferation and activity of osteoblasts [8–11] and osteoclasts [12], while radiation doses lower than 2 Gy have a stimulatory effect on osteoclast proliferation and activity [13]. Growth plate chondrocytes and bone marrow cells are the most radiation sensitive cells because of their high proliferation rate, and radiation damage to these types of cells inhibits their proliferation and thus results in growth retardation

* Corresponding author at: Laboratory of Experimental Medicine and Endocrinology, Herestraat 49, O&N1, bus 902, B-3000 Leuven, Belgium. Fax: +32 16 345 934.
E-mail address: geert.carmeliet@med.kuleuven.be (G. Carmeliet).
[1] Equal contribution.

8756-3282/$ – see front matter © 2011 Published by Elsevier Inc.
doi:10.1016/j.bone.2011.06.031

and myeloid depletion, respectively [2,14]. On the other hand, the exposure of the total mouse body to a low dose radiation of 75 mGy was found to stimulate the proliferation of bone marrow hematopoietic progenitor cells as well as their mobilization into the peripheral blood [15].

In contrast to the radiation doses used in radiation therapy, the doses associated with imaging are substantially lower. To investigate the temporal changes in bone structure during a longitudinal follow-up study, multiple successive micro-CT scans are, however, required. Frequent *in vivo* micro-CT imaging, even with relatively low radiation doses per scan, can still affect bone architecture. Discrepant results have been reported concerning the effects of micro-CT-induced radiation on the bone micro-architecture and especially the hematopoietic system in rodents. In rats, 8 weekly *in vivo* scans of 939 mGy each did not alter the structural bone parameters nor the viability of the bone marrow cells [16]. In mice, however, micro-CT-induced radiation decreased trabecular bone volume of the tibiae of 8 to 10-week old mice after 4 weekly scans with 846 mGy [17], while 4 weekly scans with 1255 mGy did not exacerbate disuse-related bone loss in the femurs of 17-week old mice [18]. It is still unclear whether this inconsistency should be attributed to differences in the radiation dose, frequency and number of *in vivo* scans or a combination of these. In addition, young, growing animals may be particularly susceptible to radiation exposure [19]. Certainly in humans, this age-related radiation sensitivity has already been thoroughly described [3].

Taken together, it is critical to delineate the settings for *in vivo* micro-CT imaging of the bone architecture of mice in order to avoid side effects on bone and hematopoietic cells that could result in altered bone structure and hematological defects. However, lowering the radiation dose to avoid radiation effects may increase noise in the images and decrease the signal-to-noise ratio, or reduce image sharpness and lower the resolution [20]. Hence, image quality needs to be weighed against the radiation risks [21]. This trade-off between dose and image quality has not been investigated thoroughly in relation to *in vivo* micro-CT imaging of mouse bone architecture. In this study, we designed 2 protocols for longitudinal micro-CT studies of the skeletal system in young pre-pubertal and adult mice that are devoid of radiation-induced side effects and maintain adequate image quality.

Materials and methods

Animals and experimental design

Male C57Bl/6 mice (Janvier) were housed under standard conditions in our animal facility (Proefdierencentrum Leuven, Belgium). All procedures were approved by the Ethical Committee of the Katholieke Universiteit Leuven.

Three types of experiments were performed: a pilot experiment, an optimisation experiment and a validation experiment. In each experiment, the left hindlimb of male C57Bl/6 mice, anesthetized with isoflurane, was scanned *in vivo* with micro-CT at 3 consecutive time points, separated each time by a 2-week interval. This follow-up period of 4 weeks was chosen because it corresponds with the evaluation period used in several murine bone pathology models such as ovariectomy, castration, tail suspension and fracture repair. The right hindlimb was positioned out of the field of view of the micro-CT and served as the non-irradiated control, as the total X-ray exposure of this hindlimb was negligible (data not shown). Following the last *in vivo* scan, mice were sacrificed by cervical dislocation and, depending on the experiment, blood was collected and the spleen, tibia and femur were isolated.

In the pilot experiment, we investigated the radiation effect of the recommended micro-CT parameters on 10-week old male C57Bl/6 mice (n = 5), an age often used as starting point in bone pathology models. The *in vivo* micro-CT parameters were 9 μm pixel size, 50 kV, 120 uA, 0.5 mm Al filter, angular rotation step 0.9°, 220 projections and an exposure time of 4.7 s with a total scan duration of 19 min. After sacrifice, dissected tibiae were imaged by *ex vivo* micro-CT after overnight fixation in 2% paraformaldehyde, and then processed for histological analysis.

In the optimization experiment, 4 and 16-week old male C57Bl/6 mice were analyzed, as age is known to change the susceptibility to radiation effects (n = 4 per age group). For each age, an additional group of mice was included, referred to as 'reference' group, and these mice were anesthetized at each time point but did not receive any *in vivo* radiation (n = 4 per age group). Two *in vivo* micro-CT parameters were used: (i) a pixel size of 9 μm (50 kV, 100 uA, 1 mm Al filter, angular rotation step 1°, 199 projections, exposure time 3.3 s, scan duration 12 min); (ii) a pixel size of 18 μm (50 kV, 100 uA, 1 mm Al filter, angular rotation step 0.8°, 248 projections, exposure time 1 s, scan duration 5 min). After sacrifice, the bone architecture was analyzed by *ex vivo* micro-CT and histology. Peripheral blood cell counts were determined and the *in vitro* colony forming capacity of hematopoietic progenitor cells of the bone marrow and spleen was analyzed. The *in vitro* osteogenic potential of bone marrow stromal cells and the differentiation of bone marrow hematopoietic cells into osteoclasts were assessed.

In the validation experiment, 10-week old male C57Bl/6 mice were either sham-operated or orchidectomized the day before the first *in vivo* micro-CT scan was taken (n = 5 per group). They were anesthetized with pentobarbitone sodium (Nembutal, 50 mg/kg body weight, CEVA Santé Animale) and received buprenorfine hydrochloride as postoperative analgesic (Temgesic, 0.05 mg/kg body weight, Schering-Plough). The *in vivo* micro-CT parameters were the 9 μm pixel size parameters used in the optimization experiment, and trabecular bone architecture was analyzed and compared between orchidectomized and sham-operated mice over time.

Micro-computed tomography

The bone micro-architecture of the tibiae was assessed *ex vivo* and *in vivo* using a SkyScan 1172 and a SkyScan 1076 micro-CT system, respectively, and related software (SkyScan). *In vivo* micro-CT images were segmented using an adaptive thresholding algorithm provided by the SkyScan CTan software because the reduced image quality precluded to use global thresholding [22]. The local threshold was calculated in a circular region of radius 8 pixels around each pixel. When indicated, registration software based on mutual information was applied to align these images [23].

The scanning parameters for *ex vivo* micro-CT imaging were 5 μm pixel size, 50 kV, 200 uA, 321 projections, 0.5 mm Al filter. After reconstruction, the *ex vivo* micro-CT images were segmented using a global threshold. The global threshold was visually determined to optimally separate the bimodal histogram into bone and soft tissue. Trabecular and cortical volumes of interest were selected manually and histomorphometric parameters were calculated according to the 'Guidelines for the assessment of bone microstructure in rodents using micro-CT' [19].

Image quality

Image quality can be quantified by severable factors such as resolution and signal-to-noise ratio. Resolution describes the ability to resolve small details in the image and can be quantified as the full-width-at-half-maximum of the system point spread function [24]. The signal-to-noise ratio in micro-CT images of the different protocols is measured as the ratio of the mean intensity over the standard deviation of the intensity in a region of interest in images of a homogeneous water phantom. More details about image quality and its relationship to radiation dose can be found in Ref. [21].

Please cite this article as: Laperre K, et al, Development of micro-CT protocols for *in vivo* follow-up of mouse bone architecture without major radiation side effects, Bone (2011), doi:10.1016/j.bone.2011.06.031

Histological analysis

Tibiae were fixed in 2% paraformaldehyde, decalcified in 0.5 M EDTA (pH 7.4)/PBS prior to dehydration, embedded in paraffin, and sectioned at 5 μm. Hematoxylin-eosin (H&E) staining and staining for tartrate-resistant acid phosphatase (TRAP) activity were performed as previously described [25,26] and were used to quantify osteoblast surface and osteoclast surface per bone surface, respectively. When indicated, bones were fixed in Burckhardt's solution, embedded undecalcified in methyl-metacrylate, sectioned at 4 μm and stained according to Von Kossa to visualize the mineralized bone matrix. Histomorphometric analysis was performed using a Zeiss Axiovert microscope and related Axiovision software (v6.1.0). Histomorphometric data were expressed according to the American Society for Bone and Mineral Research standardized histomorphometry nomenclature [27].

Radiation dose

The radiation dose was estimated by measuring the air kerma with a 0.6 cm^3 thimble ionization chamber that has a calibration factor traceable to a standard dosimetry lab (PTB, Braunschweig). The ionization chamber (type FC-65-G, IBA Dosimetry) was placed in air at the center of rotation of the scanner, resulting in an estimate of the radiation dose by means of the air kerma value.

In vitro assays

The colony forming capacity of hematopoietic progenitor cells was analyzed on bone marrow cells, flushed from the femur, and on spleen cells which were isolated by gently pressing the spleen through a 70 μm nylon mesh cell strainer (Becton Dickinson). The Methocult assay (StemCell Technologies) was performed as described before [28]. Bone marrow stromal cells isolated from tibiae and femora were cultured according to the method described previously. Osteogenic differentiation was analyzed after 2 and 3 weeks of culture by alkaline phosphatase or alizarin red staining [29]. Osteoclast formation was performed as described previously, using macrophage colony-stimulating facor (M-CSF) and receptor activator of nuclear factor kappa-B ligand (RANKL) treatment [30] and the number of TRAP-positive cells with more than three nuclei were counted as osteoclasts [31]. Cell counts (white and red blood cells and blood platelets) in peripheral blood were quantified using an Abbott Cell-Dyn 3500 hematology analyzer.

Statistics

Results are expressed as mean ± SEM, unless stated otherwise. Data were analyzed by one-way ANOVA and paired *t*-test using NCSS software (NCSS). Post hoc comparisons were performed using Fisher's least significant difference test. Differences were considered significant at $p<0.05$.

Results

In vivo micro-CT radiation doses of 776 mGy induce trabecular bone loss

To investigate whether repetitive exposure to *in vivo* micro-CT imaging, using recommended scanning parameters, might have an effect on bone architecture, we compared in a pilot experiment the bone architecture of the *in vivo* irradiated left tibia to the non-irradiated right tibia that served as control. The used scanning parameters resulted in a total radiation dose of 776 mGy per scan.

Analysis of the bone volume by *ex vivo* micro-CT imaging of the dissected tibiae showed that the *in vivo* micro-CT-induced radiation decreased trabecular bone volume by 30% in the irradiated tibia compared to the non-irradiated control tibia (Figs. 1A,B). This reduction was caused by a decrease in trabecular number (Figs. 1A,C), whereas trabecular thickness was not altered by the frequent CT scanning (Figs. 1A,D). Cortical bone mass and structure were not affected by the micro-CT-induced radiation as the total cross-sectional area (Fig. 1E), the cortical bone area (Fig. 1F) and cortical thickness (Fig. 1G) were normal.

An imbalance between osteoblast-mediated bone formation and osteoclast-mediated bone resorption is generally the cause of a decreased bone mass. Histomorphometric analysis showed that the decrease in trabecular bone volume was associated with increased bone resorption as TRAP staining revealed an increase in the osteoclast surface per bone surface in the irradiated tibiae compared to control tibiae (Fig. 1H). Bone formation, on the other hand, seemed unaltered as the osteoblast surface per bone surface, quantified on H&E stained sections, remained unchanged after *in vivo* irradiation (Fig. 1I).

These data indicate that administration of three *in vivo* micro-CT radiation doses of 776 mGy, given with a two week time interval, negatively affects bone mass in young adult mice.

Lowering the micro-CT radiation dose reduces image quality

Because the suggested scanning parameters induced radiation-related changes in bone architecture, we performed an optimization experiment in which the scanning settings were adapted in order to deliver the lowest possible radiation dose while maintaining acceptable image quality. To reduce scan duration, the angular rotation step was increased and the exposure time decreased. The current of the X-ray source was lowered and a thicker filter was used to reduce the radiation dose per unit of time. The adapted parameter set resulted in a radiation dose of 434 mGy per scan for a 9 μm pixel size scan. Further lowering of the radiation dose was achieved by combining 4 detector camera pixels to obtain an image pixel size of 18 μm, resulting in a radiation dose of 166 mGy per scan.

We first evaluated the effect of lowering the radiation dose on the quality of the obtained images. *Ex vivo* micro-CT images were taken as a reference, because the image quality achieved with this method is comparable to the one obtained in stained histological sections. Indeed, comparison between a registered *ex vivo* micro-CT image (Fig. 2A) and a von Kossa-stained histological section (Fig. 2B) revealed that the bone structures, as visualized by each of these techniques, were matching closely.

As anticipated, the quality of the *in vivo* micro-CT images was reduced when the radiation dose was decreased. Scanning with a dose of 434 mGy and a pixel size of 9 μm resulted in more blurred images compared to the *ex vivo* micro-CT scan, as demonstrated by the registration of the *ex vivo* and *in vivo* micro-CT images of the same tibia (Figs. 2C,D). Image quality was degraded even more when the bone was scanned using the protocol with a pixel size of 18 μm and a radiation dose of 166 mGy (Fig. 2E). The signal-to-noise ratio of 1.78 for the 9 μm protocol increased to 2.79 for the 18 μm pixel size protocol, while the resolution of 36 μm deteriorated to 57 μm. The slightly improved noise characteristics of the 18 μm pixel size protocol indicate that the observed quality difference can mainly be attributed to the lower resolution due to the increased pixel size. This quality difference was also reflected in the quantification of the trabecular and cortical bone parameters. *In vivo* micro-CT imaging with 18 μm, and to a lesser extent 9 μm pixel size, overestimated trabecular bone volume (Fig. 2F) and trabecular thickness (Fig. 2H) compared to *ex vivo* micro-CT imaging, but underestimated the number of trabeculae (Fig. 2G). The quantification of the cortical parameters was less influenced by the *in vivo* scanning protocols: the total cross-sectional area (Fig. 2I) and the cortical bone area (Fig. 2J) quantified from the 9 and 18 μm pixel size *in vivo* scans did not differ significantly from those quantified from the *ex vivo* scans. Similar to the trabecular

Please cite this article as: Laperre K, et al, Development of micro-CT protocols for *in vivo* follow-up of mouse bone architecture without major radiation side effects, Bone (2011), doi:10.1016/j.bone.2011.06.031

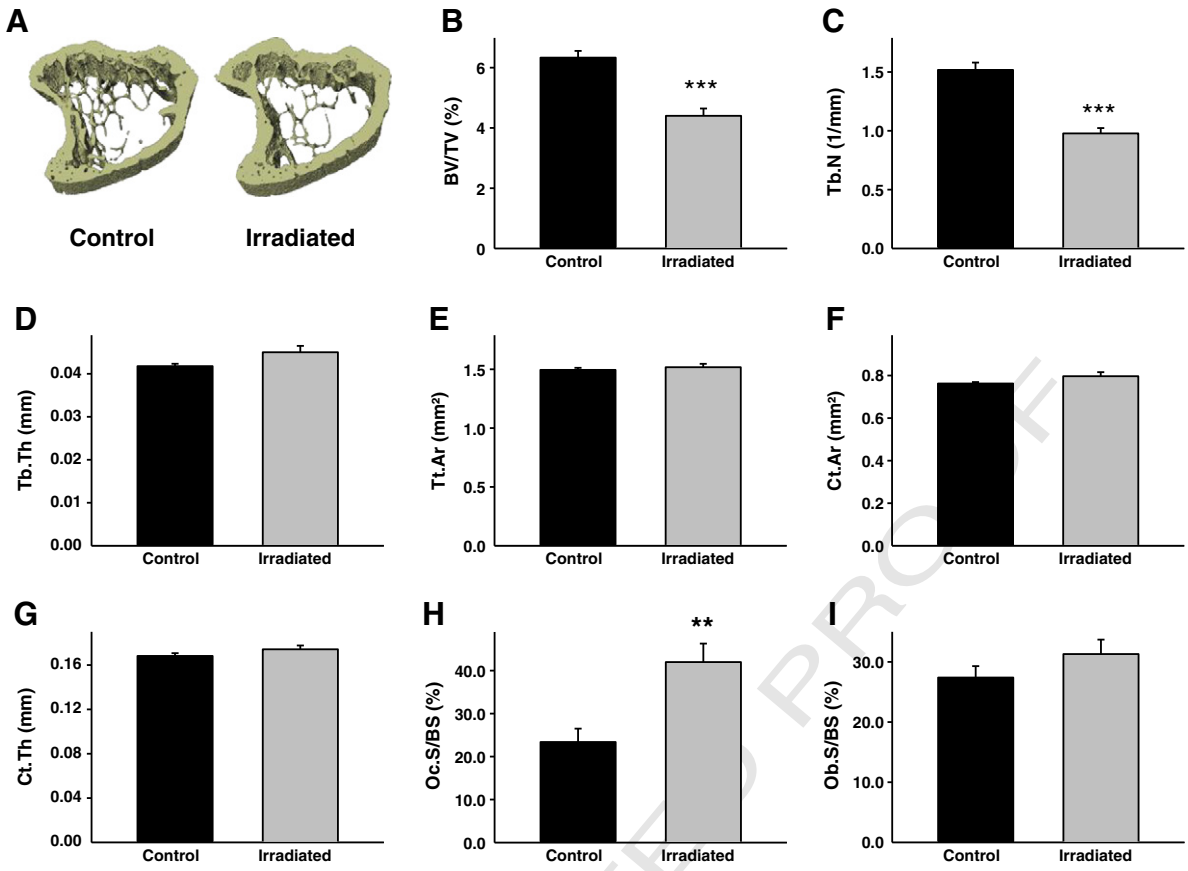

Fig. 1. Trabecular bone mass is reduced by 3 two-weekly *in vivo* micro-CT scans with a radiation dose of 776 mGy. (A) Representative 3D micro-CT images of metaphyseal bone structure of the non-irradiated right (control) and irradiated left tibia of the same mouse. (B–G) Quantification of trabecular bone volume relative to tissue volume (B; BV/TV), trabecular number (C; Tb.N), trabecular thickness (D; Tb.Th), total cross-sectional area (E; Tt.Ar), cortical bone area (F; Ct.Ar) and cortical thickness (G; Ct.Th) of the non-irradiated (control) and irradiated tibiae. (H–I) Quantification of the osteoclast surface per bone surface (H; Oc.S/BS) and osteoblast surface per bone surface (I; Ob.S/BS) on histological sections of non-irradiated (control) and irradiated tibiae after TRAP or H&E-staining, respectively. ** $p<0.01$; *** $p<0.001$ (*t*-test, *vs* control; $n=5$).

thickness, cortical thickness (Fig. 2K) was overestimated by the *in vivo* scanning protocols.

In conclusion, the two developed protocols for *in vivo* micro-CT imaging resulted in a low radiation dose, but inevitably also reduced the image quality and rendered the quantification of the bone parameters more difficult.

Bone structure is not significantly altered by repeated in vivo micro-CT imaging at a radiation dose of 434 mGy

Next, we investigated whether these adapted protocols for *in vivo* micro-CT imaging had less or even no toxic effects on trabecular and cortical bone volume. Young pre-pubertal mice (4 weeks of age) and adult mice (16 weeks of age) were subjected 3 times to one of the 2 protocols. We included the group of growing mice, since it is known that, at least in humans, young individuals are more sensitive to radiation than older persons [3]. As before, the effect of radiation on bone mass and structure was analyzed by quantifying the bone parameters in the left irradiated and right non-irradiated tibia with *ex vivo* micro-CT imaging. To avoid that interindividual variations in bone architecture between the left and right tibia masked the effect of radiation, the difference in bone parameters between the left and right tibia was calculated for each mouse and compared between the radiated group and the non-irradiated group that served as reference.

Repeated *in vivo* micro-CT imaging at 9 or 18 μm pixel size had no significant effect on the trabecular (Figs. 3A–C) or cortical (Figs. 3D–F) bone parameters, irrespective of the age of the mice, as the data were comparable to the results obtained in the non-scanned reference group. Some minor side effects of *in vivo* micro-CT radiation doses of 434 mGy (9 μm) were however detected in pre-pubertal as well as adult mice (Fig. 3A). The difference in trabecular bone volume between the left irradiated and right non-irradiated tibia was negative in every mouse, indicating that trabecular mass tended to decrease in the *in vivo* scanned tibia, although not significantly. This decrease was mainly due to a reduction in trabecular number (Fig. 3B) without an effect on trabecular thickness (Fig. 3C).

To ascertain that the effects of the 434 mGy micro-CT radiation dose on bone mass were minimal or even negligible, we analyzed osteoblast-mediated bone formation and osteoclast-mediated bone resorption. To this end, we performed histomorphometry of the irradiated and non-irradiated control tibia of pre-pubertal mice that were *in vivo* scanned at 9 μm pixel size. We reasoned that a possible negative effect of radiation would be most marked in the youngest group receiving the highest radiation dose. No significant changes were, however, observed in the osteoblast surface (Figs. 4A,B) or osteoclast surface (Figs. 4C,D) which were quantified on HE- or TRAP-stained sections, respectively. These *in vivo* findings were confirmed by *in vitro* analyses. No differences were observed in the number and size of the osteogenic colonies formed by bone marrow stromal cells derived from pre-pubertal reference mice or mice that were *in vivo* scanned at 9 μm pixel size (Fig. 5A). Furthermore, bone marrow hematopoietic cells, treated with M-CSF and RANKL, differentiated equally well to osteoclasts *in vitro* (Fig. 5B).

In summary, repeated *in vivo* exposure to micro-CT radiation doses of 434 mGy did not significantly affect bone formation or resorption, and trabecular and cortical bone parameters were thus not altered.

Please cite this article as: Laperre K, et al, Development of micro-CT protocols for *in vivo* follow-up of mouse bone architecture without major radiation side effects, Bone (2011), doi:10.1016/j.bone.2011.06.031

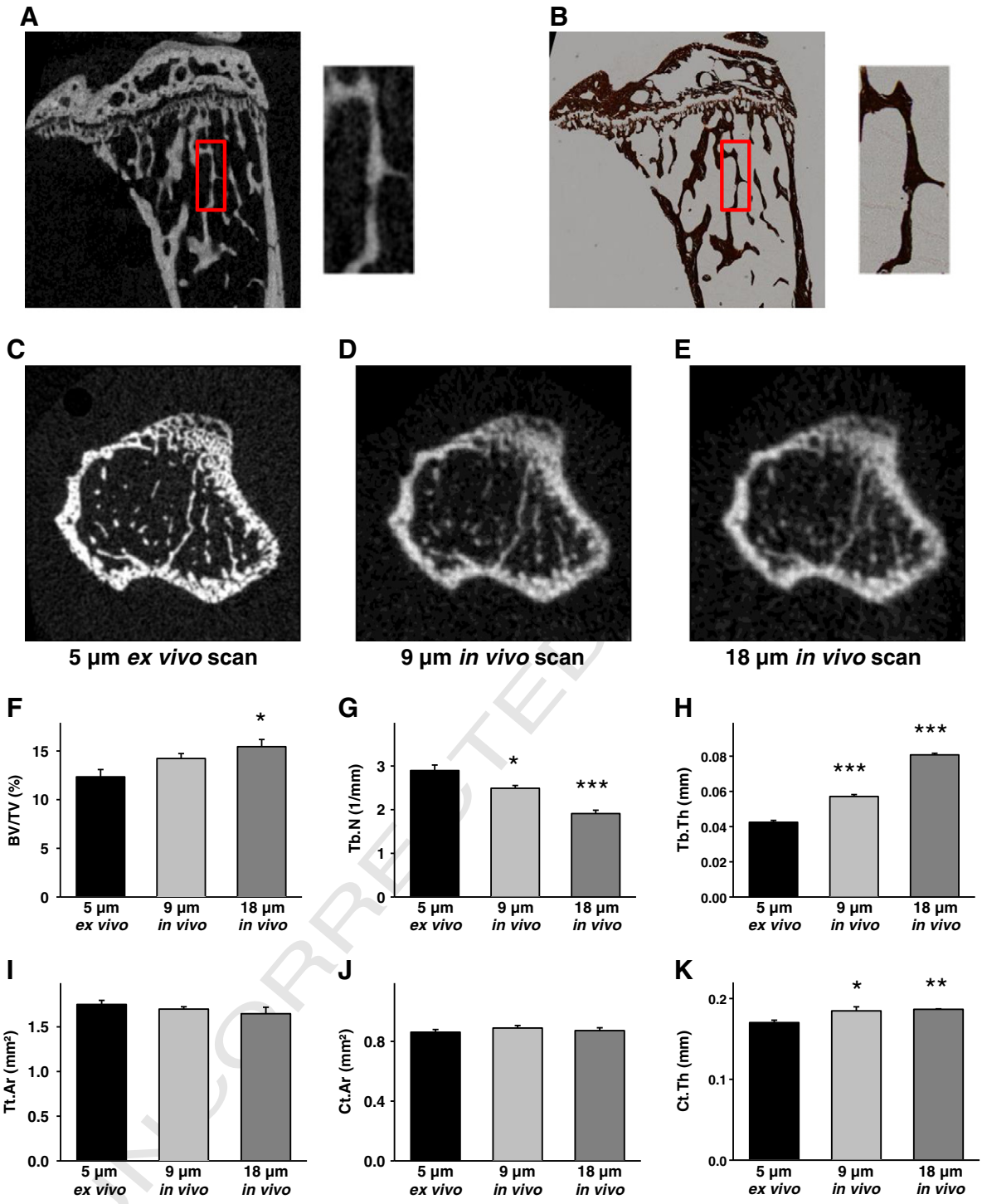

Fig. 2. Lowering the radiation dose reduces image quality. (A–B) Registered images of a tibia scanned *ex vivo* at 5 µm pixel size (A) and a Von Kossa-stained section after histological processing (B). (C–E) Registered images of the tibial metaphysis scanned *ex vivo* at 5 µm pixel size (C), *in vivo* at 9 µm pixel size (D) or *in vivo* at 18 µm pixel size (E) showing a decrease in image quality with reduced radiation dose. (F–K) Quantification of trabecular bone volume relative to tissue volume (F; BV/TV), trabecular number (G; Tb.N), trabecular thickness (H; Tb.Th), total cross-sectional area (I; Tt.Ar), cortical bone area (J; Ct.Ar) and cortical thickness (K; Ct.Th) of tibiae scanned *ex vivo* at 5 µm pixel size (black) and *in vivo* at 9 (light gray) or 18 (dark gray) micrometer pixel size. * $p<0.05$; ** $p<0.01$; *** $p<0.001$ (ANOVA, *vs* 5 µm *ex vivo* scan; $n=4$).

In vivo micro-CT radiation doses of 434 mGy are not deleterious to hematopoietic bone marrow cells

In vivo micro-CT imaging of the long bones inevitably results in radiation exposure of the bone marrow harboring the hematopoietic (stem and progenitor) cells. *In vivo* micro-CT imaging may thus indirectly influence the number of progenitors in the spleen and the number (and type) of circulating blood cells [32]. Colony forming assay of hematopoietic cells revealed that *in vivo* micro-CT imaging with 9 or 18 µm pixel size (434 or 166 mGy respectively) did not alter the number of granulocyte, macrophage or granulocyte-macrophage colony forming units in the bone marrow isolated from irradiated femora (Table 1) or in the spleen from irradiated mice (data not shown), irrespective of the age of the mice. These data are in line with

Please cite this article as: Laperre K, et al, Development of micro-CT protocols for *in vivo* follow-up of mouse bone architecture without major radiation side effects, Bone (2011), doi:10.1016/j.bone.2011.06.031

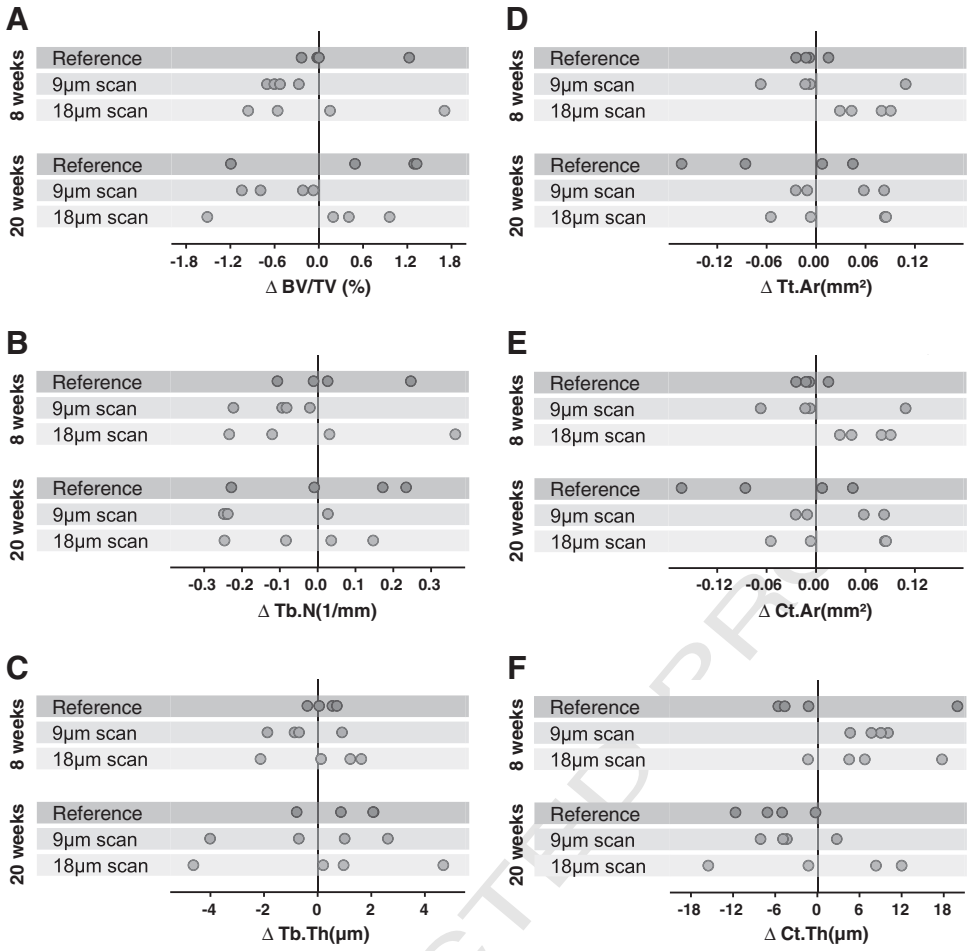

Fig. 3. Bone structure is not altered by multiple *in vivo* radiation doses of 434 mGy. The left tibia of young (8 weeks) or adult (20 weeks) mice was repetitively scanned *in vivo* at 9 or 18 µm pixel size, or not scanned (reference). The difference in trabecular and cortical bone parameters between the left and right tibia was calculated for each mouse and represented in a dot plot: difference in trabecular bone volume relative to tissue volume (A; Δ BV/TV), trabecular number (B; Δ Tb.N), trabecular thickness (C; Δ Tb.th), total cross-sectional area (D; Δ Tt.Ar), cortical bone area (E; Δ Ct.Ar) and cortical thickness (F; Δ Ct.Th) (ANOVA, *vs* reference; n = 4).

a previous report showing that *in vivo* exposure of neonatal or adult mice with a single dose of 500 mGy did not induce long-term impairment of haematopoiesis [33]. Furthermore, the number of white blood cells, red blood cells and blood platelets in peripheral blood was unaffected by the *in vivo* micro-CT radiation (Table 2).

Taken together, repetitive *in vivo* exposure to micro-CT radiation doses of up to 434 mGy did not affect hematopoietic progenitor activity.

The in vivo micro-CT imaging protocol of 434 mGy enables longitudinal follow-up of trabecular bone loss after orchidectomy

Since the developed micro-CT imaging protocols had not manifested radiation effects, we next investigated whether they were suitable to monitor changes in bone architecture during longitudinal follow-up studies (validation experiment). We therefore analyzed bone loss over time after orchidectomy, a male osteoporosis model, via *in vivo* micro-CT scanning using the 434 mGy protocol. Orchidectomy (Orx) is known to decrease trabecular bone volume, while trabecular thickness remains unchanged [34,35].

The 3D micro-CT images of the tibiae of sham-operated mice, obtained at 3 consecutive time points, showed the normal age-related decrease in trabecular bone mass (Fig. 6A). In contrast, trabecular bone volume manifestly decreased over time in orchidectomized mice (Fig. 5A). Quantification showed a 50% decrease of trabecular bone volume (Fig. 6B) and trabecular number (Fig. 6C) 2 weeks after orchidectomy and a 70% decrease of both parameters after 4 weeks. Trabecular thickness did not vary over time after orchidectomy (Fig. 6D).

In conclusion, the proposed 434 mGy micro-CT imaging protocol yields images that are of sufficient quality to quantitatively monitor changes in trabecular bone architecture over time *in vivo*.

Discussion

In vivo imaging of animals has multiple advantages, but the radiation exposure is a cause of major concern in any longitudinal *in vivo* micro-CT imaging study of the long bones of mice. Indeed, we could confirm that an ill-considered choice of micro-CT imaging parameters decreased trabecular bone mass manifestly. We therefore developed and validated two *in vivo* micro-CT imaging protocols, which are devoid of manifested radiation-induced side effects, and enabled us to quantitatively follow-up trabecular and cortical bone architecture over a 4-week period in mice.

The benefits of *in vivo* micro-CT scanning of bone architecture in mice compared to *ex vivo* imaging are patently obvious [19]. *In vivo* micro-CT imaging allows the follow-up of time-dependent changes in three-dimensional bone structure within the same animal. Registration of the sequential 3D images provides unique information on the precise sites of bone formation or bone resorption [36–38]. In addition, longitudinal studies inherently reduce the number of animals to be used. Moreover, each animal can be used as its own control, which

Please cite this article as: Laperre K, et al, Development of micro-CT protocols for *in vivo* follow-up of mouse bone architecture without major radiation side effects, Bone (2011), doi:10.1016/j.bone.2011.06.031

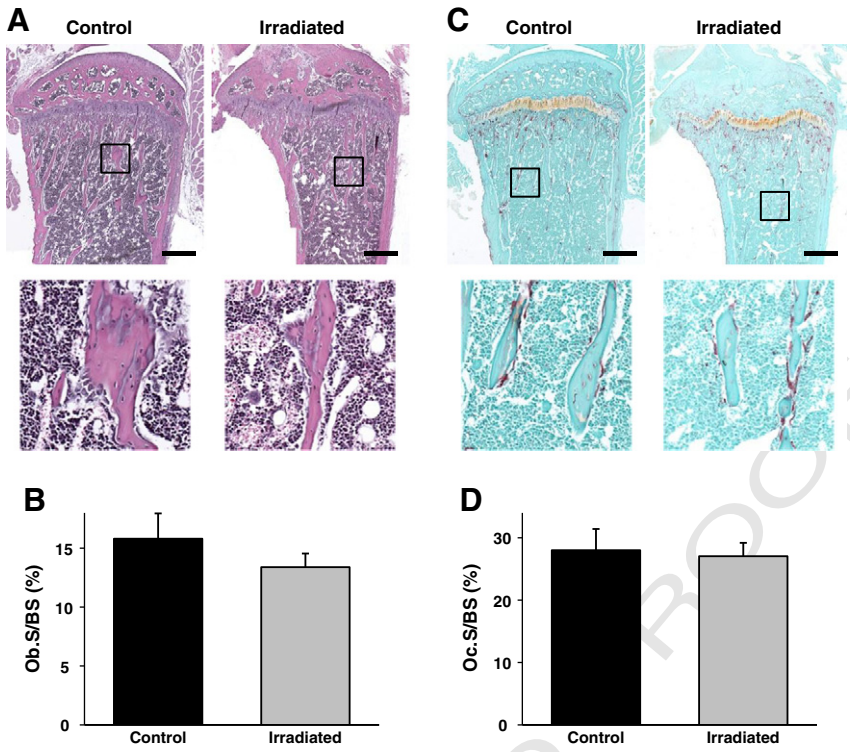

Fig. 4. Bone formation and resorption are not altered by multiple *in vivo* radiation doses of 434 mGy. (A–B) H&E staining on histological sections of the non-irradiated (control) or *in vivo* scanned tibiae (9 μm) of pre-pubertal mice (A, overview in top panel, higher magnification of boxed area in lower panel). Quantification of osteoblast surface per bone surface (B; Ob.S/BS). (C–D) TRAP-staining on histological sections of non-irradiated (control) or *in vivo* scanned tibiae (9 μm) of pre-pubertal mice (C, overview in top panel, higher magnification of boxed area in lower panel). Quantification of osteoclast surface per bone surface (D; Oc.S/BS). Bar = 500 μm. (*t*-test, *vs* control (co); n = 4).

decreases the variability and thus increases the statistical power. Possible applications are numerous and include changes in bone architecture, linked to a gene defect or caused by therapeutic intervention, besides many others. The significance and added value of these *in vivo* follow-up experiments, however, depend on the micro-CT scanning protocol that should be devoid of radiation-induced side effects. Ideally, the actual radiation dose delivered to the bone tissue should be known, but this parameter is hard to determine because it requires that the tissues surrounding the bone are simulated by a phantom. In this study, we therefore used the radiation doses measured in air (air kerma values), omitting the need for a phantom. The advantage of this approach is that these measurements are easily reproducible, which facilitates comparisons with other studies, including those referred to in this study [16,17].

We developed a 9 and 18 μm pixel size *in vivo* micro-CT imaging protocol resulting in a radiation dose of 434 mGy and 166 mGy per scan, respectively. We showed that these two protocols had no significant radiation-induced side effects on trabecular and cortical bone architecture or on the analyzed hematological parameters. The higher radiation dose tended to decrease the trabecular bone volume, but no manifested changes in bone formation or bone resorption were detected by histomorphometry, indicating that the radiation-induced effects were minimal. These *in vivo* findings were confirmed by *in vitro* analyses showing that the osteogenic differentiation of bone marrow osteoprogenitors as well as osteoclast formation from bone marrow osteoclast precursors was not reduced by the *in vivo* micro-CT scanning protocol. These findings, nevertheless, suggest that a micro-CT radiation dose of 434 mGy is close to the limit of safely using *in vivo* imaging. Indeed, repeated *in vivo* micro-CT imaging with a higher radiation dose (776 mGy in this study, 846 mGy in Ref. [17]) decreased trabecular bone volume significantly, most likely due to increased bone resorption as shown by an increase in the osteoclast abundance. It should also be noted that this limit is likely species-specific because radiation-induced toxicity was not observed in rats even with higher radiation doses. Indeed, eight *in vivo* scans with a radiation dose of 939 mGy per scan and a 1-week interval [16] or five *in vivo* scans with a radiation dose of 597 mGy and a 2-week interval [17] did not cause any changes in the bone architecture of rats.

The drawback of a reduced radiation dose is that the image quality is correspondingly decreased. As the signal-to-noise ratio obtained with the 9 μm pixel size protocol is slightly lower than that of the 18 μm pixel size protocol, the larger pixel size in the 18 μm protocol compensates for the increased noise, which is expected by the dose reduction. The apparent reduced image quality of the *in vivo* protocols can mainly be attributed to the lower resolution of the images and is manifested by blurring and intensity inhomogeneity. These effects should be taken into account by the bone segmentation process in order to minimize errors in estimates of structural bone parameters. Selecting a global threshold value to segment the bone ignores these image distortions and should be avoided as segmentation method for low-dose images. Local thresholding approaches attempt to account for intensity inhomogeneities by computing a local threshold value for every pixel, and can model blurring by adapting the thresholds in blurred regions [39]. Local thresholding methods are relatively fast and readily available, but can only handle limited image degradation. In the presence of large image degradation, such as in the images obtained with the 18 μm pixel size protocol, the local thresholding method used in this study tended to consider thin trabeculae as bone marrow because of their low intensity and the segmentation of thin trabeculae might thus fail. As a result, the number of trabeculae is likely to be underscored and the mean thickness of the trabeculae is likely to be overrated in these images. However, such segmentation errors can be considered to occur systematically within a study and therefore do not need to preclude correct relative comparisons

Please cite this article as: Laperre K, et al, Development of micro-CT protocols for *in vivo* follow-up of mouse bone architecture without major radiation side effects, Bone (2011), doi:10.1016/j.bone.2011.06.031

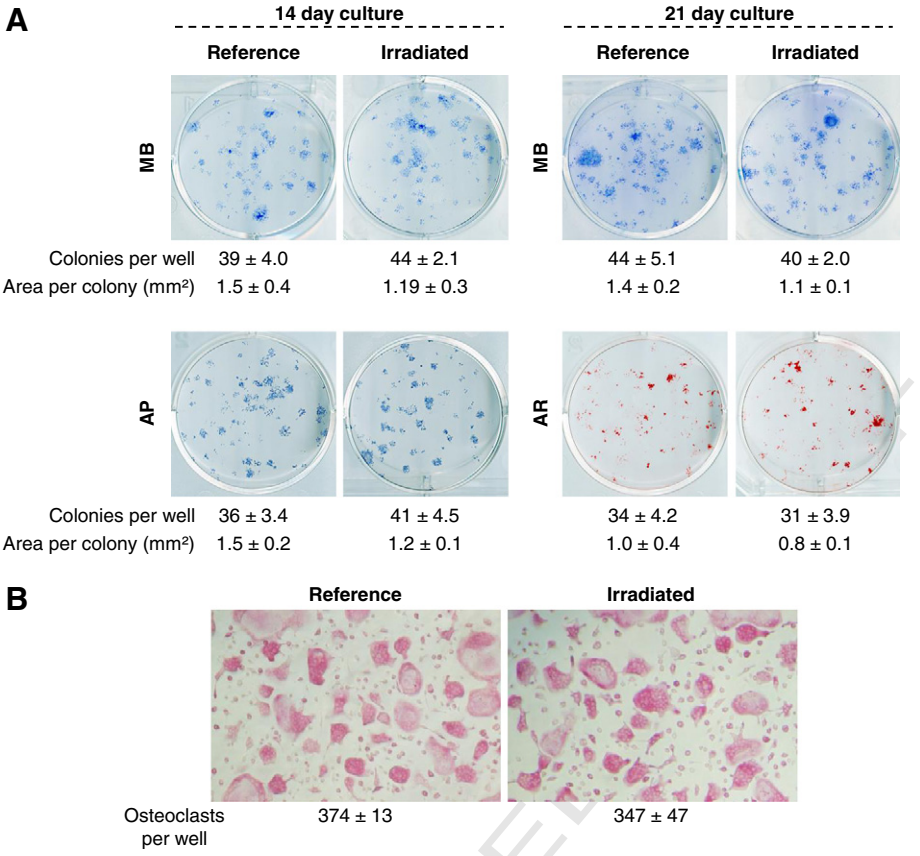

Fig. 5. Multiple *in vivo* radiation doses of 434 mGy do not affect colony forming capacity of bone marrow cells or osteoclast differentiation. (A) Representative images of methylene blue, alkaline phosphatase and alizarin red staining of bone marrow stromal cell cultures derived from non-irradiated (reference) or *in vivo* scanned tibiae (9 μm) of pre-pubertal mice after 14 or 21 days of culture with quantification of the number of osteogenic colonies per well and the average area per colony (*t*-test, *vs* reference group; n = 3). (B) Representative images of TRAP-stained osteoclasts differentiated from hematopoietic bone marrow cells derived from non-irradiated (reference) or *in vivo* scanned (9 μm) tibiae of pre-pubertal mice formed after 1 week of culture with quantification of the number of osteoclasts formed per well (*t*-test, *vs* reference group; n = 3).

between groups and over time, as has been shown in the Orx experiment. Nevertheless, care should be taken to assure that bone segmentation errors are as small as possible such that more subtle changes can be correctly detected and quantified with statistical significance. Hence, the remaining challenge for low-dose *in vivo* micro-CT imaging of bone lies in developing more sophisticated segmentation techniques to accurately extract the relevant information from the images. One such approach that is currently under investigation to overcome the limitations of traditional micro-CT segmentation techniques is the combined reconstruction and segmentation of the images [40]: rather than starting the segmentation from the degraded reconstruction, these techniques directly include the projection data in the segmentation process, allowing incorporation of the resolution properties of the scanner system and leading to more accurate segmentations.

Bearing this limitation on bone segmentation accuracy in mind, we are convinced that the image quality obtained with the proposed 9 μm pixel size *in vivo* micro-CT imaging protocol suffices for longitudinal follow-up of both trabecular and cortical bone mass and structure in mice, as demonstrated by the Orx experiment. This protocol can be applied to any experiment in which the trabecular structure of murine bone needs to be evaluated. Extracting accurate quantitative information on trabecular parameters from images acquired with the proposed 18 μm pixel size *in vivo* micro-CT imaging protocol is less likely. Yet, the 18 μm pixel size protocol has its merit in its much lower radiation dose compared to the 9 μm pixel size protocol and may allow more frequent imaging. Hence, it might be more suited to

Table 1
Colony forming capacity of bone marrow hematopoietic cells.

Age	Colony type	Reference	9 μm *in vivo* scan	18 μm *in vivo* scan
8 weeks	CFU-G	17.5 ± 0.9	14.8 ± 2.7	17.8 ± 1.7
	CFU-M	18.5 ± 2.4	15.3 ± 2.7	15.0 ± 0.7
	CFU-GM	13.5 ± 12.5	12.3 ± 1.7	12.5 ± 1.5
	Total CFU	49.0 ± 4.8	42.3 ± 5.4	45.3 ± 2.4
20 weeks	CFU-G	16.3 ± 3.4	18.0 ± 1.9	21.3 ± 1.9
	CFU-M	17.0 ± 4.7	16.8 ± 3.0	18.8 ± 2.2
	CFU-GM	14.3 ± 3.4	13.5 ± 2.2	15.3 ± 1.9
	Total CFU	47.5 ± 11.2	48.3 ± 5.2	55.3 ± 4.9

Number of granulocyte (G), macrophage (M) and granulocyte-macrophage (GM) colony forming units (CFU) per 10^4 bone marrow cells isolated from femora of 8- or 20-week-old mice that were not *in vivo* scanned (reference) or scanned at 9 or 18 μm pixel size. (ANOVA, *vs* reference; n = 4).

Table 2
Peripheral blood cell and platelet counts.

Age	Colony type	Reference	9 μm *in vivo* scan	18 μm *in vivo* scan
8 weeks	WBC ($\times 10^3$/μl)	2.4 ± 0.4	2.5 ± 0.5	3.0 ± 0.3
	RBC ($\times 10^3$/μl)	9.4 ± 0.1	9.2 ± 0.2	9.2 ± 0.3
	BPL ($\times 10^3$/μl)	1580 ± 20.1	1530 ± 27.8	1471 ± 55.2
20 weeks	WBC ($\times 10^3$/μl)	2.6 ± 0.5	2.7 ± 0.5	2.2 ± 0.4
	RBC ($\times 10^3$/μl)	9.1 ± 0.2	8.8 ± 0.1	7.9 ± 0.7
	BPL ($\times 10^3$/μl)	1516 ± 92.2	1428 ± 99.3	961 ± 190.9

Number of white blood cells (WBC), red blood cells (RBC) and blood platelets (BPL) in peripheral blood isolated from 8- or 10-week-old mice that were not *in vivo* scanned (reference) or scanned at 9 or 18 μm pixel size. (ANOVA, *vs* reference; n = 4).

Please cite this article as: Laperre K, et al, Development of micro-CT protocols for *in vivo* follow-up of mouse bone architecture without major radiation side effects, Bone (2011), doi:10.1016/j.bone.2011.06.031

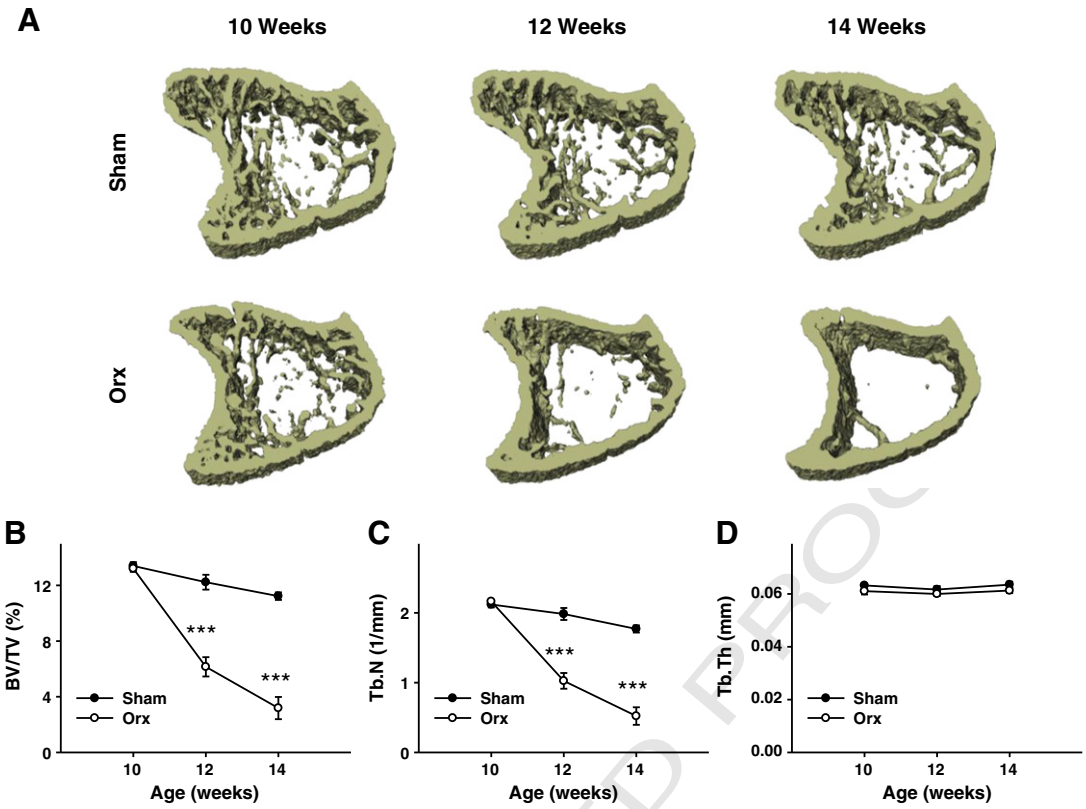

Fig. 6. The 9 μm *in vivo* micro-CT imaging protocol enables longitudinal follow-up of trabecular bone loss after orchidectomy. (A) 3D micro-CT models of the metaphysis of sham-operated (Sham) or orchidectomized mice (Orx), analyzed by *in vivo* micro-CT imaging at the time of the operation (10 weeks of age) or 2 (12 weeks of age) and 4 weeks (14 weeks of age) after the procedure. (B–D) Quantification of trabecular bone volume relative to tissue volume (B; BV/TV), trabecular number (C; Tb.N) and trabecular thickness (D; Tb.Th). *** $p<0.001$ (*t*-test, *vs* Sham; $n=4–5$).

monitor manifested changes in bone mass and structure such as callus formation during fracture repair or large bone lesions associated with bone metastasis progression.

In conclusion, *in vivo* micro-CT is a useful tool for the *in vivo* follow-up of bone mass and structure in mice. However, proper optimization of the scan parameters and study set-up is necessary, as high radiation doses can alter bone morphological parameters. We here provide two study set-ups for the *in vivo* follow-up of both young and old mice over a study period of 4 weeks without significant side effects of *in vivo* X-ray exposure.

Acknowledgments

The authors thank I. Stockmans, R. Van Looveren, F. Callewaert and E. Van Herck (Katholieke Universiteit Leuven) for their assistance. This work was supported by a grant from the Fund for Scientific Research-Flanders (FWO: G.0569.07 and G.0500.08), the Molecular Small Animal Imaging Centre (MoSAIC) and IWT SBO project Quantiviam (060819). K. Laperre and N. Van Gastel are fellows of the Institute for the Promotion of Innovation through Science and Technology in Flanders (IWT-Vlaanderen).

Appendix A. Supplementary data

Supplementary data to this article can be found online at doi:10.1016/j.bone.2011.06.031.

References

[1] Jiang Y, Zhao J, White DL, Genant HK. Micro CT and micro MR imaging of 3D architecture of animal skeleton. J Musculoskelet Neuronal Interact 2000;1:45–51.
[2] Williams HJ, Davies AM. The effect of X-rays on bone: a pictorial review. Eur Radiol 2006;16:619–33.
[3] Mitchell MJ, Logan PM. Radiation-induced changes in bone. Radiographics 1998;18:1125–36 [quiz 1242–3].
[4] Hutchinson F. The molecular basis for radiation effects on cells. Cancer Res 1966;26:2045–52.
[5] Olive PL, Banath JP, Durand RE. Heterogeneity in radiation-induced DNA damage and repair in tumor and normal cells measured using the "comet" assay. Radiat Res 1990;122:86–94.
[6] Iliakis G, Wang Y, Guan J, Wang H. DNA damage checkpoint control in cells exposed to ionizing radiation. Oncogene 2003;22:5834–47.
[7] Song S, Lambert PF. Different responses of epidermal and hair follicular cells to radiation correlate with distinct patterns of p53 and p21 induction. Am J Pathol 1999;155:1121–7.
[8] Dudziak ME, Saadeh PB, Mehrara BJ, Steinbrech DS, Greenwald JA, Gittes GK, et al. The effects of ionizing radiation on osteoblast-like cells in vitro. Plast Reconstr Surg 2000;106:1049–61.
[9] Matsumura S, Jikko A, Hiranuma H, Deguchi A, Fuchihata H. Effect of X-ray irradiation on proliferation and differentiation of osteoblast. Calcif Tissue Int 1996;59:307–8.
[10] Dare A, Hachisu R, Yamaguchi A, Yokose S, Yoshiki S, Okano T. Effects of ionizing radiation on proliferation and differentiation of osteoblast-like cells. J Dent Res 1997;76:658–64.
[11] Gal TJ, Munoz-Antonia T, Muro-Cacho CA, Klotch DW. Radiation effects on osteoblasts in vitro: a potential role in osteoradionecrosis. Arch Otolaryngol Head Neck Surg 2000;126:1124–8.
[12] Scheven BA, Burger EH, Kawilarang-de Haas EW, Wassenaar AM, Nijweide PJ. Effects of ionizing irradiation on formation and resorbing activity of osteoclasts in vitro. Lab Invest 1985;53:72–9.
[13] Willey JS, Lloyd SA, Robbins ME, Bourland JD, Smith-Sielicki H, Bowman LC, et al. Early increase in osteoclast number in mice after whole-body irradiation with 2 Gy X rays. Radiat Res 2008;170:388–92.
[14] Huang W, Yang Y, Sun Z, Zeng X. Early radiation-induced bone marrow injury: serial MR imaging during initial 4 weeks after irradiation. Acad Radiol 2009;16:733–8.
[15] Li W, Wang G, Cui J, Xue L, Cai L. Low-dose radiation (LDR) induces hematopoietic hormesis: LDR-induced mobilization of hematopoietic progenitor cells into peripheral blood circulation. Exp Hematol 2004;32:1088–96.
[16] Brouwers JE, van Rietbergen B, Huiskes R. No effects of in vivo micro-CT radiation on structural parameters and bone marrow cells in proximal tibia of wistar rats detected after eight weekly scans. J Orthop Res 2007;25:1325–32.

Please cite this article as: Laperre K, et al, Development of micro-CT protocols for *in vivo* follow-up of mouse bone architecture without major radiation side effects, Bone (2011), doi:10.1016/j.bone.2011.06.031

[17] Klinck RJ, Campbell GM, Boyd SK. Radiation effects on bone architecture in mice and rats resulting from in vivo micro-computed tomography scanning. Med Eng Phys 2008;30:888–95.
[18] Judex S, Chung H, Torab A, Xie L, Rubin C, Donahue L, et al. Micro-CT induced radiation does not exacerbate disuse related bone loss. Proceedings of the 51st annual meeting of the orthopaedic research society; 2005.
[19] Bouxsein ML, Boyd SK, Christiansen BA, Guldberg RE, Jepsen KJ, Muller R. Guidelines for assessment of bone microstructure in rodents using micro-computed tomography. J Bone Miner Res 2010;25:1468–86.
[20] Ford NL, Thornton MM, Holdsworth DW. Fundamental image quality limits for microcomputed tomography in small animals. Med Phys 2003;30:2869–77.
[21] Goldman LW. Principles of CT: radiation dose and image quality. J Nucl Med Technol 2007;35:213–25 [quiz 226–8].
[22] Kuhn JL, Goldstein SA, Feldkamp LA, Goulet RW, Jesion G. Evaluation of a microcomputed tomography system to study trabecular bone structure. J Orthop Res 1990;8:833–42.
[23] Maes F, Collignon A, Vandermeulen D, Marchal G, Suetens P. Multimodality image registration by maximization of mutual information. IEEE Trans Med Imaging 1997;16:187–98.
[24] Judy PF. The line spread function and modulation transfer function of a computed tomographic scanner. Med Phys 1976;3:233–6.
[25] Maes C, Stockmans I, Moermans K, Van Looveren R, Smets N, Carmeliet P, et al. Soluble VEGF isoforms are essential for establishing epiphyseal vascularization and regulating chondrocyte development and survival. J Clin Invest 2004;113:188–99.
[26] Maes C, Carmeliet P, Moermans K, Stockmans I, Smets N, Collen D, et al. Impaired angiogenesis and endochondral bone formation in mice lacking the vascular endothelial growth factor isoforms VEGF164 and VEGF188. Mech Dev 2002;111:61–73.
[27] Parfitt AM, Drezner MK, Glorieux FH, Kanis JA, Malluche H, Meunier PJ, et al. Bone histomorphometry: standardization of nomenclature, symbols, and units. Report of the ASBMR Histomorphometry Nomenclature Committee. J Bone Miner Res 1987;2:595–610.
[28] Maes C, Coenegrachts L, Stockmans I, Daci E, Luttun A, Petryk A, et al. Placental growth factor mediates mesenchymal cell development, cartilage turnover, and bone remodeling during fracture repair. J Clin Invest 2006;116:1230–42.
[29] Masuyama R, Stockmans I, Torrekens S, Van Looveren R, Maes C, Carmeliet P, et al. Vitamin D receptor in chondrocytes promotes osteoclastogenesis and regulates FGF23 production in osteoblasts. J Clin Invest 2006;116:3150–9.
[30] Lieben L, Benn BS, Ajibade D, Stockmans I, Moermans K, Hediger MA, et al. Trpv6 mediates intestinal calcium absorption during calcium restriction and contributes to bone homeostasis. Bone 2010;47:301–8.
[31] Daci E, Udagawa N, Martin TJ, Bouillon R, Carmeliet G. The role of the plasminogen system in bone resorption in vitro. J Bone Miner Res 1999;14:946–52.
[32] Kopp HG, Avecilla ST, Hooper AT, Rafii S. The bone marrow vascular niche: home of HSC differentiation and mobilization. Physiology (Bethesda) 2005;20:349–56.
[33] Grande T, Bueren JA. Analysis of hematopoiesis in mice irradiated with 500 mGy of X rays at different stages of development. Radiat Res 1995;143:327–33.
[34] Li M, Jee WS, Ke HZ, Tang LY, Ma YF, Liang XG, et al. Prostaglandin E2 administration prevents bone loss induced by orchidectomy in rats. J Bone Miner Res 1995;10:66–73.
[35] Erben RG, Eberle J, Stahr K, Goldberg M. Androgen deficiency induces high turnover osteopenia in aged male rats: a sequential histomorphometric study. J Bone Miner Res 2000;15:1085–98.
[36] Boyd SK, Moser S, Kuhn M, Klinck RJ, Krauze PL, Muller R, et al. Evaluation of three-dimensional image registration methodologies for in vivo micro-computed tomography. Ann Biomed Eng 2006;34:1587–99.
[37] Nishiyama KK, Campbell GM, Klinck RJ, Boyd SK. Reproducibility of bone micro-architecture measurements in rodents by in vivo micro-computed tomography is maximized with three-dimensional image registration. Bone 2009;46:155–61.
[38] Waarsing JH, Day JS, van der Linden JC, Ederveen AG, Spanjers C, De Clerck N, et al. Detecting and tracking local changes in the tibiae of individual rats: a novel method to analyse longitudinal in vivo micro-CT data. Bone 2004;34:163–9.
[39] Waarsing JH, Day JS, Weinans H. An improved segmentation method for in vivo microCT imaging. J Bone Miner Res 2004;19:1640–50.
[40] Depypere M, Nuyts J, Laperre K, Carmeliet G, Maes F, Suetens P. The minimal entropy prior for simultaneous reconstruction and segmentation of in vivo microCT trabecular bone images. 2009 IEEE international symposium on biomedical imaging: from nano to macro, Vols 1 and 2; 2009. p. 586–9.

Please cite this article as: Laperre K, et al, Development of micro-CT protocols for *in vivo* follow-up of mouse bone architecture without major radiation side effects, Bone (2011), doi:10.1016/j.bone.2011.06.031